Thermal performance of Eco-Friendly Mortars with Recycled Aggregates and Supplementary Materials

by T. Cardinale*, F. Grandizio*, A. Feo*, C. Sposato*, A. Saponaro**, D. Lorenzo**

* *ENEA, Italian National Agency for New Technologies, Energy and Sustainable Economic Development, Trisaia Research Centre, S.S. 106 Ionica, Km 419+500, Rotondella (MT), 75026, Italy*
tiziana.cardinale@enea.it
* *ENEA, Italian National Agency for New Technologies, Energy and Sustainable Economic Development, Trisaia Research Centre, S.S. 106 Ionica, Km 419+500, Rotondella (MT), 75026, Italy*
francesco.grandizio@enea.it
* *ENEA, Italian National Agency for New Technologies, Energy and Sustainable Economic Development, Trisaia Research Centre, S.S. 106 Ionica, Km 419+500, Rotondella (MT), 75026, Italy*
andrea.feo@enea.it
* *ENEA, Italian National Agency for New Technologies, Energy and Sustainable Economic Development, Trisaia Research Centre, S.S. 106 Ionica, Km 419+500, Rotondella (MT), 75026, Italy*
corradino.sposato@enea.it
** *ENEA, Italian National Agency for New Technologies, Energy and Sustainable Economic Development, Brindisi Research Centre, S.S. 7 Appia, km 706, Brindisi, 72100, Italy*
andrea.saponaro@enea.it
** *ENEA, Italian National Agency for New Technologies, Energy and Sustainable Economic Development, Brindisi Research Centre, S.S. 7 Appia, km 706, Brindisi, 72100, Italy*
daniela.lorenzo@enea.it

Abstract

This study investigates the energy-related and mechanical behaviour of eco-friendly cementitious mortars containing waste materials, with particular attention to the replacement of cement with natural pozzolan and of aggregates with autoclaved aerated concrete (AAC) and end-of-life tire rubber (ELT). Thermal diffusivity was evaluated using a modified Parker-based method with active infrared thermography. The results show that AAC–ELT mixtures exhibit significantly lower thermal diffusivity than conventional cementitious mortars, with reductions of up to approximately 60%, while binder replacement has only a limited influence on the thermal response. A general relationship between thermal diffusivity and the mechanical performance of the investigated mixtures was also observed.

1. Introduction

In recent years, the growing demand for sustainable and high-performance construction materials has driven significant research efforts toward the development of innovative cement-based composites with enhanced thermal and environmental properties. In this context, the characterization of thermophysical properties, such as thermal diffusivity, plays a fundamental role in understanding heat transfer mechanisms and optimizing the energy performance of building envelopes.

Infrared thermography (IRT) has emerged as a powerful non-destructive technique for the evaluation of thermal behaviour in materials, offering the advantage of full-field, contactless measurements and enabling the analysis of transient heat transfer processes. Active thermography approaches, in particular, allow the quantitative determination of thermal properties through controlled thermal excitation and subsequent monitoring of surface temperature evolution. These techniques have been increasingly applied to cement-based materials for both defect characterization and thermophysical property estimation, demonstrating their potential for reliable and efficient material assessment.

Among the various methodologies, the flash method originally proposed by Parker [1] has been widely adopted for the evaluation of thermal diffusivity, due to its simplicity and effectiveness. However, real experimental conditions often deviate from the ideal assumptions of instantaneous and one-dimensional heat transfer. In this regard, finite pulse effects and heat losses, first addressed by Cape and Lehman [2], must be considered to obtain accurate estimations of this thermophysical parameter. Subsequent developments have further refined these approaches, adapting them to practical experimental setups and extending their applicability to different material systems.

At the same time, increasing attention has been devoted to the use of recycled materials in cementitious composites, to reduce environmental impact and promote circular economy strategies. End-of-life tire (ELT) rubber has been widely investigated as a partial replacement of natural aggregates, leading to the development of rubberized concretes and mortars. The incorporation of rubber particles generally results in a modification of the microstructure, characterized by increased porosity and the presence of hydrophobic phases, which significantly affect both

License: https://creativecommons.org/licenses/by/4.0/deed.en

mechanical and transport properties. Specifically, it has been demonstrated that the addition of rubber aggregates leads to a reduction in thermal conductivity and diffusivity, improving the thermal insulation behaviour of the material.

From a microstructural perspective, the transport properties of cement-based materials are strongly governed by pore structure, connectivity, and density. More compact and homogeneous systems typically exhibit higher thermal diffusivity and mechanical strength, due to a more continuous solid phase that facilitates heat propagation. Conversely, the introduction of lightweight and porous phases, such as AAC or rubber aggregates, alters the heat transfer pathways, resulting in reduced effective thermal transport.

Although AAC-based materials and rubberized cementitious composites have been extensively investigated separately [3, 4, 5, 6], their combined influence on thermal diffusivity, particularly when assessed through active infrared thermography techniques, remains limited.

In this framework, the present study aims to investigate the thermal diffusivity of innovative cement-based mortars incorporating autoclaved aerated concrete (AAC) and ELT rubber through an active infrared thermography approach. The analysis is based on a modified Parker method applied to the transient thermal response obtained from controlled heating experiments. In addition, the relationship between thermal behaviour and material composition is explored, with particular attention to the influence of microstructure, moisture content, and mechanical performance. The experimental results provide insights into the role of recycled aggregates in tailoring the thermal response of cementitious materials, contributing to the development of more energy-efficient and sustainable construction solutions.

2. Materials and Methods

2.1. Concrete mix design and samples preparation

The investigated samples consisted of cementitious mortar formulations with different mix designs, including a reference mix (3:1), a pozzolanic mix with 35% cement substitution, AAC-based mixtures, AAC–ELT (end-of-life tire rubber) mixtures, and AAC combined with natural sand. Among these, only the 100% AAC mixtures were prepared using both 3:1 and 4:1 aggregate-to-binder ratios, whereas all the other formulations, although not explicitly specified, were produced using the 3:1 ratio. The detailed composition and identification of the samples are reported in table 1.

Table 1. *Sample identification and composition details*

Sample ID	Mix design	Average thickness [mm]
2025_07_16 REF 3:1_1	REF 3:1	23
2025_07_16 REF 3:1_2	REF 3:1	23
2025_07_16 POZZ 35%_1	35% POZZOLANIC	24
2025_07_16 POZZ 35%_2	35% POZZOLANIC	24
2025_07_08_A1	100% AAC (REF 3:1)	23
2025_07_08_A2	100% AAC (REF 3:1)	23
2025_07_08_B1	100% AAC (REF 4:1)	23.5
2025_07_08_B2	100% AAC (REF 4:1)	23
2025_07_08_C1	95% AAC 5% ELT	23
2025_07_08_C2	95% AAC 5% ELT	22
2025_07_08_D1	90%AAC 10% ELT	24
2025_07_08_D2	90%AAC 10% ELT	24
2025_07_08_E1	70%AAC 30% ELT	23.5
2025_07_08_E2	70%AAC 30% ELT	23.5
2025_07_17 AAC 90%_1	90% AAC 10% natural sand	23
2025_07_17 AAC 90%_2	90% AAC 10% natural sand	24
2025_07_17 ELT 90%_1	90% ELT 10% natural sand	24.5
2025_07_17 ELT 90%_2	90% ELT 10% natural sand	25

For each formulation, two replicate prismatic samples were prepared (see table 1) to ensure the repeatability of the experimental measurements. The results reported in the following sections are based on the average values of the replicated samples.

The samples were initially weighed in their wet state (figure 1(a)). Drying was performed in a ventilated oven at 50 °C for up to 72 h (figure 1(b)), according to the standard UNI EN 1015-10:2007 [7], that provides a dry temperature of 105±5 °C, not applicable for cementitious specimens containing polymer waste. The mass of each specimen was monitored at 24 h intervals, with intermediate measurements performed after cooling the samples to ambient

temperature to ensure stable readings. The drying process was considered complete when mass variations between consecutive measurements became negligible.

Mass loss was evaluated as the difference between initial and final mass, while the percentage variation was calculated with respect to the initial mass according to Eq. (1):

$$\Delta m\% = \frac{m_{wet} - m_{dry}}{m_{wet}} * 100 \qquad (1)$$

Where m_{wet} is the initial wet mass and m_{dry} is the final mass after drying.

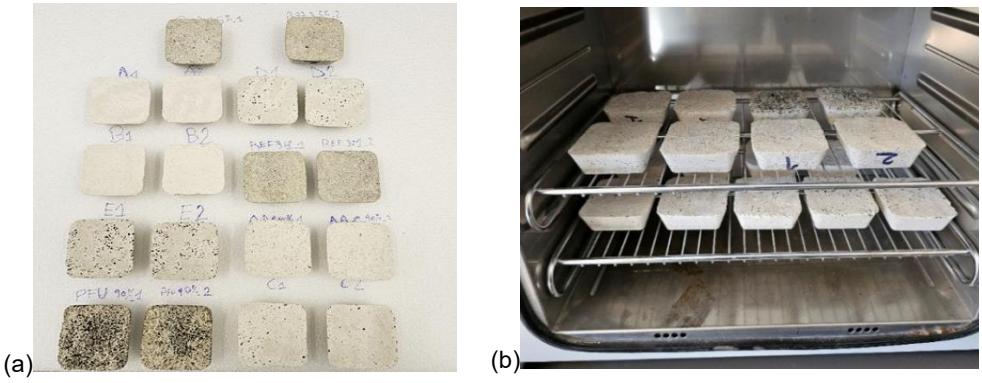

(a) (b)

Figure 1. Sample preparation and drying process: (a) specimens before drying, (b) oven at 50 °C

2.2. Experimental setup for thermal measurements

Thermal diffusivity measurements were carried out using a transmission-mode setup based on active thermographic inspection, as shown in figure 2.

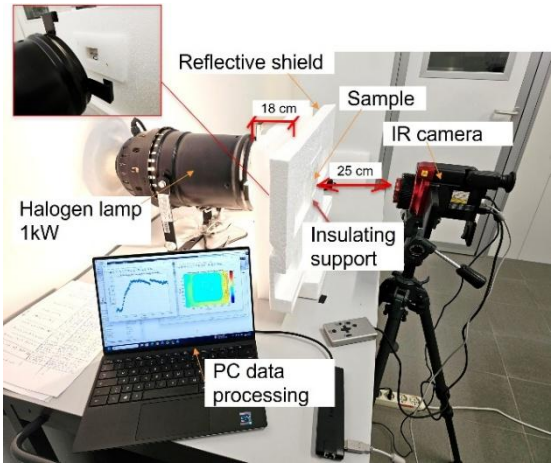

Figure 2. Experimental setup for thermal measurements in transmission mode

The system consisted of a 1000 W halogen lamp used as a controlled heat source, an infrared (IR) camera (model Avio 550) with a resolution of 640×480 pixels, and a low-emissivity aluminium shield designed to reflect thermal radiation after the lamp was switched off, thereby minimizing environmental interference. Following several preliminary tests to optimize the experimental configuration, the distance between the sample and the halogen lamp was set to 18 cm, while the distance between the sample and the IR camera was fixed at 25 cm (figure 2).

During testing, each sample was heated from one side for 40 s while the temperature evolution was recorded on the opposite surface using the IR camera. Thermal images were acquired every 3 s over a total duration of 1200 s. The emissivity was set to 0.92, consistently with typical values reported for cement-based materials in infrared thermography studies [8]. Prior to each test, samples were conditioned to reach a uniform initial temperature.

2.3. Thermal data acquisition and processing

The acquired thermal data were processed using a custom algorithm developed in MATLAB 2011b. An example of the data processing procedure is shown for sample 2025_07_08_C1.

The thermal analysis is based on the one-dimensional transient heat conduction equation [9, 10] (Eq. (2)):

$$\frac{\partial T}{\partial t} = \alpha \frac{\partial^2 T}{\partial x^2} \tag{2}$$

Where T is the temperature, t is the time, x is the spatial coordinate, and α is the thermal diffusivity. A region of interest (ROI) was defined on the thermal map, selected on an arbitrary frame, as illustrated in figure 3(a). The custom routine computes the mean temperature within the selected ROI over the entire acquisition, from the initial frame to the end of the recording. This procedure allows the extraction of the temperature evolution as a function of time (figure 3(b)), yielding the temperature–time curves used for subsequent analysis.

In the temperature–time graph, the absolute time corresponds to the elapsed time from the beginning of the acquisition, while the relative time is defined with respect to the onset of heating on the opposite face of the sample, immediately after activation of the halogen lamp.

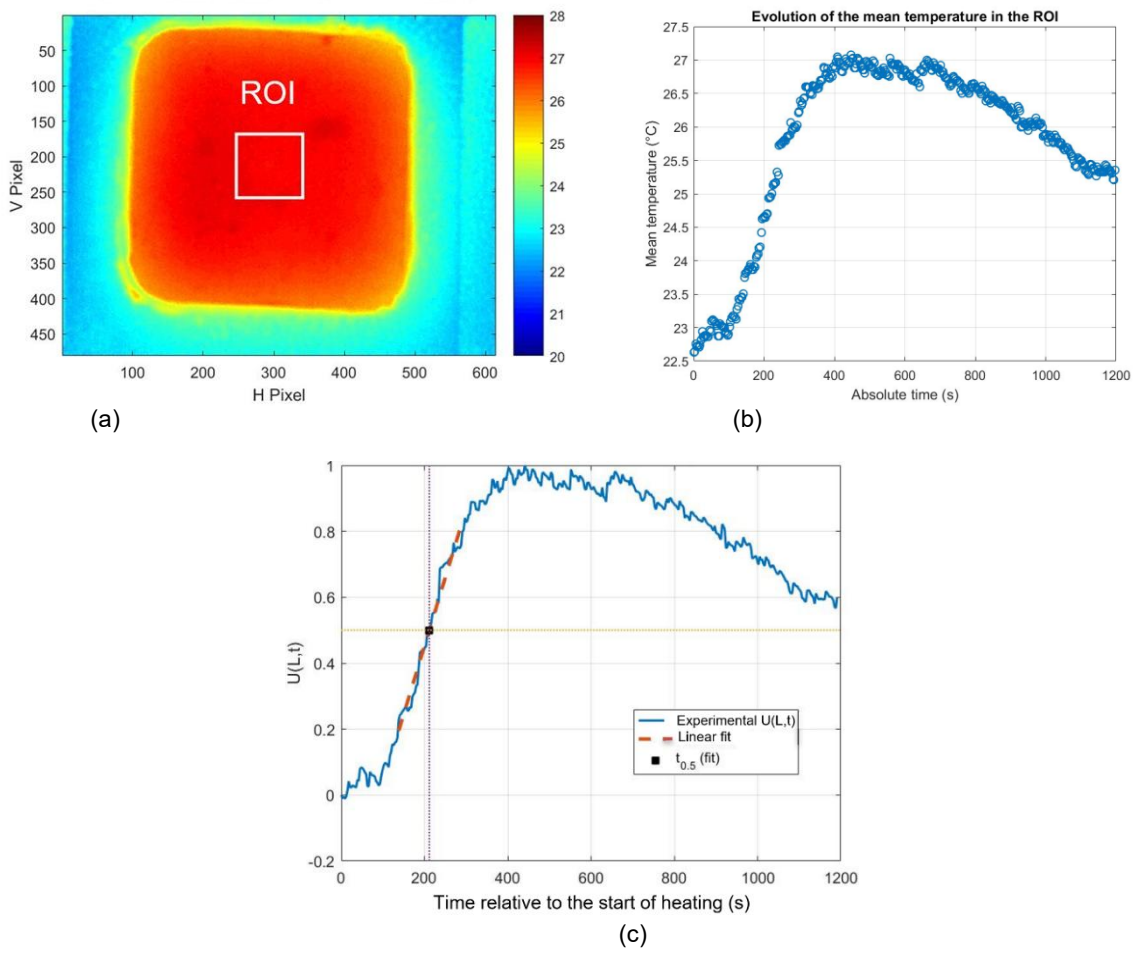

Figure 3. (a) ROI selection; (b) mean temperature over time; (c) diffusivity from Parker method

The thermal diffusivity of the mortar samples was evaluated using a modified version of the Parker method [1] with non-impulsive heating, similarly to the approach adopted in [11, 12, 13], where a halogen lamp is used as the heat source and the analysis is based on the transient response of the rear surface temperature [1, 2, 14, 15, 16, 17].

The normalized temperature rise U (L, t) was obtained from the temperature–time curves (Figure 3(c)) and is expressed as [1, 18]:

$$U(L,t) = \frac{\Delta T(L,t)}{\Delta T_{max}} = 1 + 2\sum_{n=1}^{\infty} (-1)^n e^{-n^2\omega} \tag{3}$$

Where ΔT (L, t) is the temperature rise of the rear surface of the sample at time t, defined as the difference between the instantaneous surface temperature and the initial uniform temperature of the sample prior to heating. ΔT_{max} is the maximum temperature increase measured during the transient.

The dimensionless parameter ω is defined as [1]:

$$\omega = \frac{\pi^2 \alpha t}{L^2} \tag{4}$$

Where α is the thermal diffusivity, t_{is} the time, and L is the sample thickness. Starting from this formula (Eq. (4)), the thermal diffusivity can be evaluated using the Parker model, which relates the characteristic time of the thermal response to the material properties and geometry of the sample. This approach is commonly used in non-destructive evaluations where thermal diffusivity is required for quantitative analysis of material properties and defect characterization [13]. In this framework, the thermal diffusivity is expressed as [1, 2, 18, 19]:

$$\alpha = \frac{W_x L^2}{\pi^2 t_x} \tag{5}$$

where Wx is a dimensionless constant that depends on the selected reference fraction of the temperature rise, L is the sample thickness, and tx is the time required for the sample to reach a given fraction of the maximum temperature increase (typically 50%). According to [1, 2], for $t_{1/2}$, the corresponding constant is $W_{1/2}$ = 1.370.

The data processing algorithm implemented in this work is based on the analytical scheme shown in figure 3(c), which allows the extraction of the characteristic time from the experimental thermal response curves and its subsequent use for the calculation of thermal diffusivity.

3. Results and discussion

3.1. Drying process behaviour and mass loss analysis

The evolution of mass during the drying process is reported in figure 4(a, b). Data are reported as mean values obtained from independent replicate samples.

As observed in figure 4(a), all samples exhibit a consistent drying behaviour characterized by a rapid initial decrease in mass, followed by a progressive reduction in the drying rate until a quasi-stationary condition is reached.

This trend reflects a typical two-stage drying mechanism, consistently with drying behaviour reported for cement-based materials in controlled conditions [20]: an initial phase governed by the evaporation of free water from the surface, and a subsequent phase controlled by moisture diffusion from the internal pore structure toward the exterior.

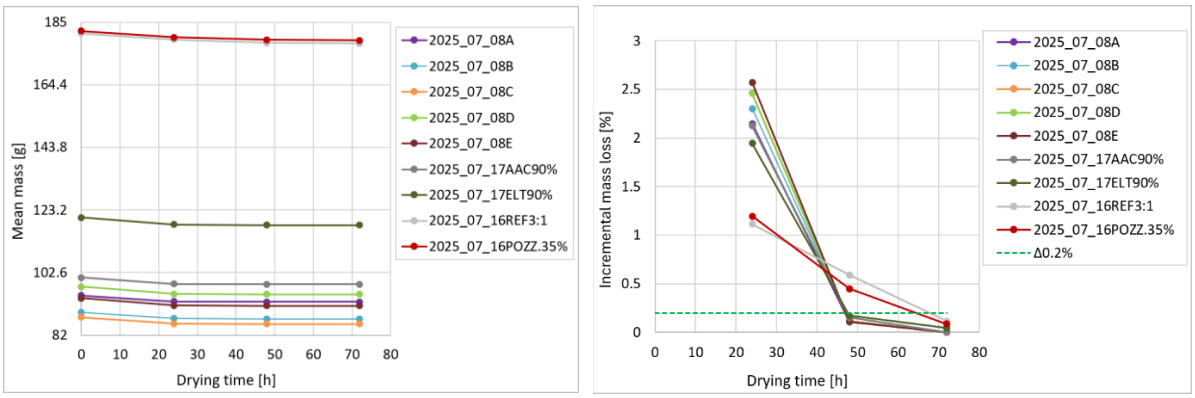

(a) (b)

Figure 4. Drying behaviour of the samples: (a) mass evolution during drying and (b) incremental mass loss (%) between successive measurements

The interpretation of this behaviour is further supported by figure 4(b), where the incremental mass loss (%) between successive measurements was evaluated according to Eq. 6.

$$\Delta m_i\% = \frac{m_{i-1} - m_i}{m_{i-1}} * 100 \tag{6}$$

Where m_{i-1} and m_i represent the specimen mass measured at two consecutive drying intervals.

Since no mass variation occurs at the initial condition (t = 0 h), the incremental analysis starts from the first drying interval (0–24 h), and the initial zero point was omitted from the plot for clarity. Similar approaches based on incremental mass change during drying have been reported in the literature for cement-based materials [20].

The results show that the highest incremental mass loss occurs during the first drying interval (0–24 h). After this stage, the rate of mass change significantly decreases, indicating a transition from surface-controlled evaporation to diffusion-limited transport. The flattening of the curves in both figures confirms that the system progressively approaches equilibrium moisture conditions.

This behaviour is further highlighted in figure 4(b) by a dashed line indicating the 0.2% threshold, commonly adopted as an equilibrium criterion for mass stabilization, in accordance with the relevant standard ASTM C1792 [21].

Differences among the investigated formulations become evident when comparing both the absolute mass loss (figure 4(a)) and the incremental mass loss (figure 4(b), table 2). In particular, the reference AAC samples (100% AAC) exhibit a faster initial mass reduction, suggesting a higher fraction of easily removable moisture and a more open and interconnected pore network that facilitates moisture transport. Conversely, mixtures containing ELT show a more gradual and delayed mass loss. This behaviour can be attributed to the hydrophobic nature of the polymeric fraction, which limits water mobility and reduces capillary transport within the matrix.

The total mass loss (%) of the investigated samples, obtained from replicate measurements, is reported in table 2 as mean values.

Table 2. *Total mass loss of the investigated samples (mean values)*

Mix design	Initial mass [g]	Final mass [g]	Total mass loss [%]
REF 3:1	181.30	178.05	1.79
35% POZZ	182.20	179.05	1.73
100% AAC (REF 3:1)	95.05	92.95	2.21
100% AAC (REF 4:1)	89.45	87.30	2.41
95% AAC + 5% ELT	87.85	85.65	2.51
90% AAC + 10% ELT	97.90	95.45	2.50
70% AAC + 30% ELT	94.15	91.70	2.61
90% AAC + 10% sand	100.95	98.70	2.23
90% ELT + 10% sand	120.75	118.20	2.12

Samples incorporating natural sand exhibit an intermediate behaviour, likely due to modifications in pore size distribution and overall permeability. These microstructural features influence both the rate and extent of moisture removal, as reflected in the different slopes and final values of the curves.

From a quantitative perspective, the mass variation values reported in table 2, expressed as mean ± standard deviation, indicate a relatively limited removable moisture content across all samples. Although the differences among mixtures are moderate, they are consistent with the observed drying kinetics and confirm the role of mix design in governing water retention and transport properties.

Finally, all samples reach a near-stable condition after approximately 48–72 hours (see Figure 4a and Figure 4b), indicating that equilibrium moisture conditions are approached under the applied drying regime. The residual mass differences among formulations further highlight the combined effect of porosity, connectivity, and material composition on the drying process.

Overall, the drying behaviour highlights the key role of mix design and microstructure in governing moisture transport within the investigated materials. The observed differences in mass loss kinetics can be directly related to variations in pore structure and connectivity, which are known to strongly influence moisture diffusion in cement-based systems [22, 23]. In addition, the presence of hydrophobic phases such as ELT further affects water mobility and retention, as rubber particles can modify the interaction between the solid matrix and liquid water, limiting liquid ingress despite increasing porosity [24].

These aspects are expected to significantly influence not only the drying process but also the thermal response of the materials under transient conditions. In particular, the same microstructural features controlling moisture transport are closely linked to heat transfer mechanisms, as porosity, phase distribution, and internal connectivity directly affect thermal diffusivity.

Therefore, the analysis of the thermal response and the estimation of thermal diffusivity provide complementary information, allowing a deeper understanding of the relationship between material composition, moisture behaviour, and heat transfer performance.

3.2. Thermal response and diffusivity assessment

The thermal response of the investigated samples, processed using a 10-point moving average, is reported in figure 5(a, b), where the temporal evolution of the average temperature and the normalized temperature rise U (L, t) are shown for all mix designs.

As observed in figure 5(a), all samples exhibit a consistent thermal behaviour characterized by a rapid increase in average temperature during the initial heating phase (approximately within the first 200–300 s). This stage is associated with the onset of surface heating and the establishment of a thermal gradient within the material. After this initial transient, the temperature evolution progressively slows down, reaching a quasi-steady condition

A similar trend is observed in figure 5(b), where the normalized temperature rise U (L, t) rapidly increases in the early stages and tends to stabilize between approximately 400 and 700 s, reaching values typically in the range of 0.85–0.95 depending on the mixture. This plateau corresponds to the establishment of a dominant conductive heat transfer regime, in which the system progressively approaches thermal equilibrium conditions.

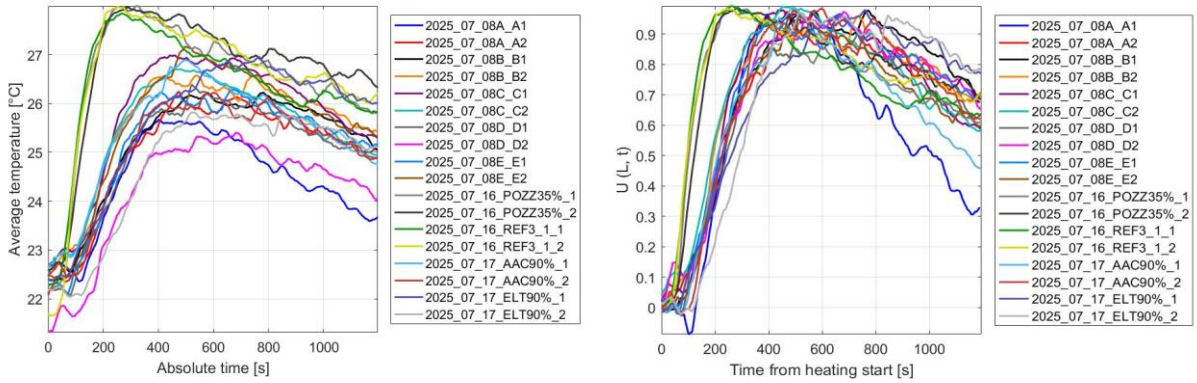

(a) (b)

Figure 5. Time evolution of the thermal response for all samples processed with a 10-point moving average: (a) average temperature and (b) normalized temperature increase U (L, t)

For longer times (beyond approximately 800–900 s), a slight decrease in the normalized response is observed for several samples. This behaviour can be attributed to non-ideal effects, such as lateral heat losses and deviations from the ideal one-dimensional heat transfer assumption adopted in the analytical model, as commonly reported in active thermography due to heat losses, multidimensional effects and boundary condition deviations [10].

Despite these minor deviations, the overall response remains consistent across all materials, confirming the reliability and repeatability of the experimental procedure, as commonly required and evaluated in active thermographic measurements through repeatability and reproducibility analyses [25].

Clear differences among mix compositions emerge when comparing the thermal responses. Samples containing increasing amounts of ELT (70% AAC – 30% ELT and 90% ELT-10% sand mixtures) exhibit a progressively slower thermal response, with slightly lower values of U (L, t) in the final part of the transient and a delayed attainment of the plateau condition. This indicates a reduction in effective heat transfer efficiency in AAC–ELT mixtures compared to conventional cementitious systems, maybe due to the combined effect of increased porosity and the low thermal conductivity of the rubber phase. This behaviour is reflected in the estimated thermal diffusivity values, which remain close to approximately 3.3×10^{-7} m²/s for the 70% AAC – 30% ELT mixture, while slightly decreasing for the 90% ELT formulation. The values of all investigated samples, expressed as mean, are summarized in table 3. These results suggest that ELT incorporation contributes to reducing heat propagation compared to conventional cementitious systems, leading to a more thermally resistive behaviour under transient conditions, as widely reported for rubberized cement-based materials, where the addition of rubber particles decreases thermal conductivity and enhances thermal insulation properties [26, 27, 28].

A more detailed comparison within the AAC-based systems shows that the reference mixtures (100% AAC REF 3:1 and REF 4:1) exhibit very similar thermal behaviour, as reported in table 3.

Table 3. *Thermal diffusivity values obtained from repeated measurements. Values are reported as mean*

Mix design	Thermal diffusivity α [×10⁻⁷ m²/s]
100% AAC (REF 3:1)	3.208
100% AAC (REF 4:1)	3.499
95% AAC + 5% ELT	3.495
90% AAC + 10% ELT	3.357
70% AAC + 30% ELT	3.382
90% AAC + 10% sand	3.407
90% ELT + 10% sand	3.083
REF 3:1	7.597
POZZ 35%	7.134

The corresponding curves are well overlapped, indicating good repeatability and consistency of the experimental measurements. Similarly, mixtures containing limited ELT content (approximately 90–95% AAC) exhibit thermal diffusivity values comparable to those of 100% AAC samples (3.3–3.5 × 10^{-7} m²/s), with their thermal response curves remaining within the main AAC behaviour cluster. These results suggest that low ELT additions (up to about 10%) do not significantly affect the effective thermal diffusivity, as heat transfer remains predominantly governed by the AAC matrix.

In contrast, reference cement-based materials (REF 3:1 and POZZ 35%) exhibit significantly higher thermal diffusivity values compared to AAC-based mixtures (see Table 3). AAC-based systems exhibit thermal diffusivity values approximately 50–60% lower than conventional cementitious reference mortars, indicating a slower heat propagation and improved thermal insulating behaviour. Their thermal response curves are characterized by a faster increase in U (L, t) and a more rapid attainment of higher normalized temperature levels, indicating more efficient heat propagation within the material.

Overall, the comparison highlights a clear distinction between conventional cementitious systems and AAC-based composites. While traditional materials are characterized by higher thermal diffusivity and faster heat transfer, AAC–ELT mixtures exhibit reduced diffusivity and slower thermal response, confirming their improved insulating performance under transient thermal conditions.

4. Relationship between thermal and mechanical properties

A relationship between thermal diffusivity and mechanical performance can be observed across the investigated mixtures. This relationship is analysed in terms of compressive strength (figure 6(a)) and flexural strength (figure 6(b)).

A qualitative relationship is observed between thermal diffusivity and compressive strength (figure 6(a)). In general, the REF and pozzolanic-based systems exhibit significantly higher compressive strength together with higher thermal diffusivity, indicating a more compact and continuous microstructural structure. This behaviour is consistent with previous studies, where thermal transport properties in cement-based materials are strongly governed by pore structure, connectivity and overall material density [23]. In contrast, AAC-based composites show lower mechanical performance and reduced variability in thermal diffusivity.

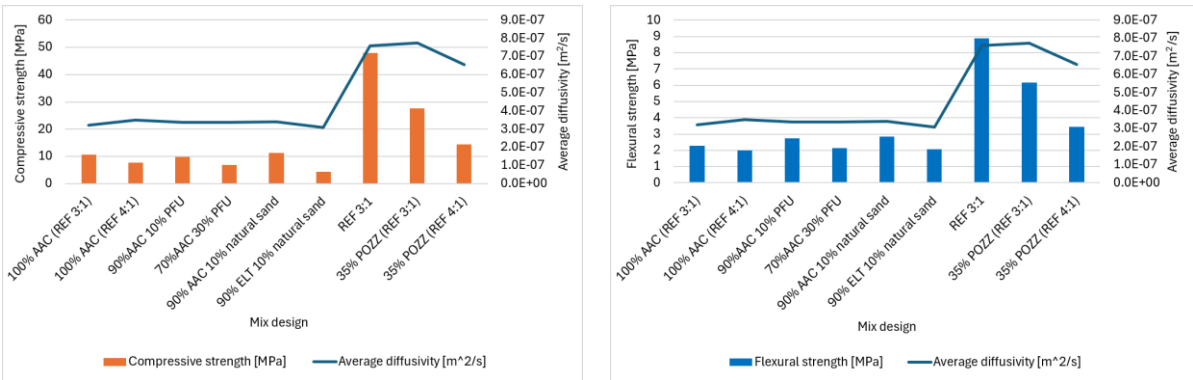

(a) (b)

Figure 6. Correlation between (a) thermal diffusivity and compressive strength and (b) thermal diffusivity and flexural strength for the investigated mortars

Within this context, AAC- and ELT-based mixtures exhibit relatively low thermal diffusivity values, indicating improved insulating performance. However, this enhancement in thermal behaviour is achieved at the expense of mechanical properties, which are generally lower than those of the reference and more compact mixtures.

Among the AAC-based mixtures, the incorporation of natural sand leads to a slight increase in compressive strength, suggesting a densification effect within the matrix. Conversely, ELT-containing mixtures exhibit reduced compressive strength, while only minor variations in thermal diffusivity are observed, indicating a partial decoupling between thermal and mechanical behaviour.

A similar trend is observed for flexural strength (figure 6(b)). REF and POZZ systems again show superior performance compared to AAC-based composites, while ELT-modified mixtures display reduced flexural strength. The ELT–sand mixture exhibits the lowest mechanical performance among the AAC-based systems, confirming the weakening effect of the polymeric phase on structural integrity.

Overall, the results suggest that thermal diffusivity is primarily governed by the continuity of the solid phase, whereas mechanical properties are more sensitive to compositional modifications and pore structure variations. These findings highlight a partial coupling between thermal and mechanical behaviour, strongly influenced by mix design and microstructural development.

5. Conclusions

This study investigated the thermo-physical behaviour of a range of eco-friendly mortars, including AAC-based formulations, with particular focus on the influence of ELT (end-of-life tire rubber), natural sand, and alternative binders on coupled moisture and heat transport properties. The experimental approach, combining drying tests and thermal diffusivity measurements based on active infrared thermography in transmission mode, enabled the establishment of a consistent link between microstructural characteristics and macroscopic performance [10, 29]. The obtained results are in line with previous studies on thermographic characterization of cement-based materials, further confirming the reliability of active infrared techniques for the quantitative evaluation of thermal properties in heterogeneous systems [8, 11].

The results demonstrate that the drying process is strongly affected by the mix design. AAC-based mixtures exhibit a faster initial mass loss, associated with higher water availability and a more interconnected pore network. Conversely, the incorporation of ELT leads to a slower drying behaviour, which can be attributed to the hydrophobic nature of rubber particles, potentially limiting water mobility within the matrix. Mixtures containing natural sand show an intermediate response, confirming the key role of particle size distribution and pore structure in governing moisture transport mechanisms.

From a thermal perspective, diffusivity measurements obtained using the transmission configuration indicate that AAC and AAC–ELT mixtures exhibit relatively low and comparable values for low ELT contents (up to 10%), suggesting a limited influence of the polymer phase when the AAC matrix remains dominant. However, the presence of ELT generally results in slower heat propagation and a more pronounced insulating behaviour compared to conventional cementitious systems, consistent with a reduced efficiency of transient heat transfer through the material [27, 28]. In contrast, conventional cementitious mixtures (REF 3:1 and pozzolanic systems) exhibit significantly higher thermal diffusivity values, confirming their greater ability to transfer heat due to a denser and more continuous solid microstructure.

These findings highlight a clear relationship between microstructure, polymer content, and thermo-hygrometric behaviour, where increased compactness is associated with enhanced heat transfer, while the introduction of lightweight or hydrophobic phases promotes thermal insulation [22, 28]. Overall, the incorporation of ELT modifies the material response by reducing heat propagation and enhancing thermal insulation properties, while simultaneously influencing moisture release kinetics.

These results suggest that AAC–ELT mixtures can be effectively tailored for building applications aimed at improving energy efficiency, where the balance between moisture management and thermal insulation represents a critical design parameter.

Future developments will focus on a more detailed microstructural characterization, including porosimetric analyses, as well as on the evaluation of thermo-hygrometric behaviour under realistic environmental conditions, in order to further validate the applicability of these materials in practical building scenarios.

Acknowledgements

The authors gratefully acknowledge Sabbie di Parma SRL and Bacchi S.p.A., through Giuseppe Ruggiero and Andrea Riva, for their valuable technical support and for providing the raw materials necessary to carry out the experimental activities. Their contribution was made within the framework of the ENEA Proof of Concept (PoC 2023) project GECO – Green Ecolight Cement mOrtar (Det. N. 239/2024/TERIN, 29 October 2024, Act Code: PZ1AAG TERIN202307), coordinated by Tiziana Cardinale.

References

[1] W. J. Parker, R. J. Jenkins, C. P. Butler e G. L. Abbott, «Flash method of determining thermal diffusivity, heat capacity, and thermal conductivity, » Journal of Applied Physics, vol. 32, pp. 1679–1684, 1961.

[2] J. A. Cape and G. W. Lehman, «Temperature and finite pulse-time effects in the flash method for measuring thermal diffusivity, » Journal of Applied Physics, vol. 34, pp. 1909–1913, 1963.

[3] A. B. Alengaram, M. Z. Jumaat, H. Mahmud, “Influence of aggregate replacement by waste rubber on thermal properties of concrete,” Construction and Building Materials, 2013.

[4] T. Q. Tran, B. S. Thomas, W. Zhang, et al., “A comprehensive review on treatment methods for end-of-life tire rubber used for rubberized cementitious materials,” Construction and Building Materials, vol. 359, 2022, 129365.

[5] M. Jerman, M. Keppert, J. Černý, “Hygric, thermal and durability properties of autoclaved aerated concrete,” Construction and Building Materials, vol. 41, 2013, pp. 352–359.

[6] D. Zhang, “Previous and present investigations on autoclaved aerated concrete – A review,” Construction and Building Materials, vol. 135, 2017, pp. 505–516.

[7] UNI EN 1015-10:2007 Methods of test for mortar for masonry - Part 10: Determination of dry bulk density of hardened mortar.

[8] E. Barreira, R.M.S.F. Almeida e M.L Simões, «Emissivity of Building Materials for Infrared Measurements, » Sensors vol. 21, article number 1961, 2021.

[9] H. S. Carslaw and J. C. Jaeger, «Conduction of Heat in Solids, » 2nd ed., Oxford, UK: Oxford University Press, 1959.

[10] D.R. Poirier e G.H.Geiger, «Conduction of Heat in Solids, »in Transport Phenomena in Materials Processing. The Minerals, Metals & Materials Series. Springer, Cham, 2016.

[11] B. Milovanović e I. Banjad Pečur, «Review of Active IR Thermography for Detection and Characterization of Defects in Reinforced Concrete, » J. Imaging, vol. 2, article number 11, 2016.

[12] R. Krankenhagen, F. Jonietz e S. Zirker, «Determination of Thermal Parameters of Concrete by Active Thermographic Measurements, » J. Nondestruct. Eval. vol. 41, article number 25, 2022.

[13] B. Milovanović and I. Banjad Pečur, «Using infrared thermography for thermal diffusivity testing of concrete, » in Proceedings of 17th Quantitative InfraRed Thermography Conference (QIRT 2024), Zagreb, Croatia, 2024.

[14] R. D. Cowan, «Pulse method of measuring thermal diffusivity at high temperatures, » Journal of Applied Physics, vol. 34, pp. 926–927, 1963.

[15] Y. Tao, L. Yang, Q. Zhong, Z. Xu e C. Luo, «Note: A method for correction of finite pulse time effects in flash diffusivity measurements of thin films, » Rev. Sci. Instrum., vol. 87, article number 086104, 2016.

[16] R. Sundar e C. Sudha, «Thermal Transport and Thermal Diffusivity by Laser Flash Technique: A Review, » Int. J. Thermophys vol. 46, article number 13, 2025.

[17] Z. Ali, S.Addepalli and Y. Zhao, «Effective Thermal Diffusivity Measurement Using Through-Transmission Pulsed Thermography: Extending the Current Practice by Incorporating Multi-Parameter Optimisation, » Sensors, vol. 25, article number 1139, 2025.

[18] A. Salazar, D. Sagarduy-Marcos, J. Rodríguez-Aseguinolaza, A. Mendioroz, J. C. Ciria e R. Celorrio, «Resolution of Multiple Semi-Infinite Delaminations Using Lock-In Infrared Thermography, » NDT & E International, vol. 146, article number 103156, 2024.

[19] UNI EN ISO 18755:2023, Fine ceramics (advanced ceramics, advanced technical ceramics) - Determination of thermal diffusivity of monolithic ceramics by flash method (ISO 18755:2022).

[20] M. Segawa, A. Aili, I. Maruyama, «Comparison of shrinkage and mass change of hardened cement paste under gradual drying and rapid drying, » Cement, vol. 10, p. 100047, 2022.

[21] ASTM C1792-14, «Standard Test Method for Measurement of Mass Loss Versus Time for One-Dimensional Drying of Saturated Concretes, » ASTM International, 2014.

[22] O.H.A. Dehwah, H. Hamidane e Y. Xi, «Characterization of effective moisture diffusivity based on pore structure of concrete, » Sci. Rep. 14, article number 18450, 2024.

[23] Z. Luo e L. Jiao, «Experimental, computational, and simulation methods for investigating the pore connectivity of cement-based materials: a review, » Front. Mater. vol.12, article number 1664496, 2025.

[24] R. Di Mundo, A. Petrella e M. Notarnicola, «Surface and bulk hydrophobic cement composites by tyre rubber addition, » Construction and Building Materials, vol. 172, pp. 176-184, 2018.

[25] M. Švantner, L.Muzika, A. Moskovchenko, C.M.C. Pereira e S. Das. «Repeatability Study of Flash-Pulse Thermographic Inspection of CFRP Samples, » Eng. Proc., vol. 8, article number 1, 2021.

[26] A. Cojocaru, D.N. Isopescu, S.G. Maxineasa e S.G.Petre, «Assessment of Thermal and Mechanical Properties of Cement-Based Materials—Part 1: Crumb Rubber Concrete, » Buildings, vol.13, article number 324, 2023.

[27] Y.C. Khern, S.C. Paul, S.Y. Kong, A.J. Babafemi, V. Anggraini, M.J. Miah e B. Šavija, «Impact of Chemically Treated Waste Rubber Tire Aggregates on Mechanical, Durability and Thermal Properties of Concrete, » Front. Mater., vol. 7, article number 90, 2020.

[28] E. Ghorbel, S. Omary e A. Karrech, «Recovered Tire-Derived Aggregates for Thermally Insulating Lightweight Mortars, » Materials, vol.18, article number 1849, 2025.

[29] H. Kim, N. Lamichhane, C. Kim, R. Shrestha, «Innovations in Building Diagnostics and Condition Monitoring: A Comprehensive Review of Infrared Thermography Applications, » Buildings vol.13, article number 2829, 2023.